

---

# RAT 🐹 : Bridging RNN Efficiency and Attention Accuracy via Chunk-based Sequence Modeling

---

Xiuying Wei<sup>1\*</sup>, Anunay Yadav<sup>1</sup>, Razvan Pascanu<sup>2</sup>, Caglar Gulcehre<sup>1</sup>  
<sup>1</sup>CLAIRE, EPFL <sup>2</sup>Google DeepMind

## Abstract

Transformers have become the cornerstone of modern large-scale language models, but their reliance on softmax attention poses a computational bottleneck at both training and inference. Recurrent models offer high efficiency, but compressing the full sequence into a fixed-size and holistic representation suffers from memory degradation in long contexts and limits fine-grained retrieval. To address this, we propose RAT, an intermediate design that bridges the efficiency of RNNs and capacity of attention. RAT partitions the input into chunks, applies recurrence within each chunk for local dependencies, and softmax-based attention across chunks for long-range interactions. This design mitigates memory degradation and enables direct access to distant tokens, while retaining computational efficiency. Empirically, with a chunk size of 16, the RAT block achieves a  $7\times$  improvement in training speed with 100K token sequences and  $9\times$  in generation at the 4K position, while maintaining similar performance compared to standard attention. We demonstrate this by training 1.3B parameter models from scratch and performing large-scale evaluations, including short- and long-context benchmarks, as well as supervised finetuning (SFT). We further propose a hybrid architecture that interleaves RAT with local attention. By combining efficient long-range modeling with strong local interactions, this hybrid design not only improves inference speed and reduces cache memory usage, but also consistently enhances performance and shows the overall best results. Code is available at <https://github.com/CLAIRE-Labo/RAT>.

## 1 Introduction

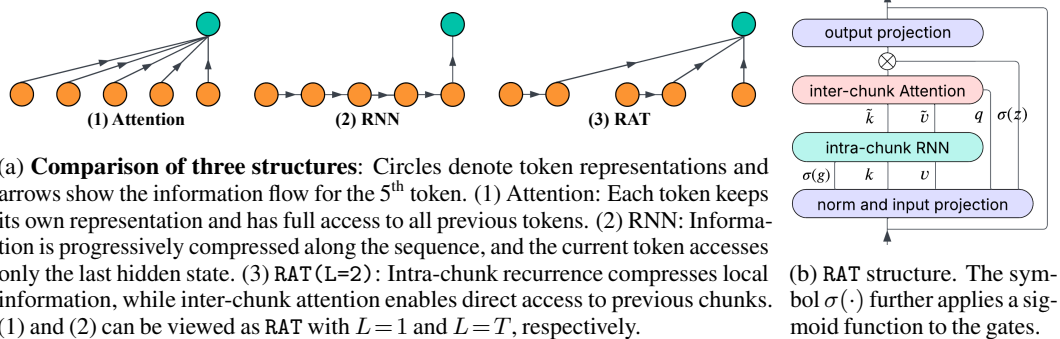
Language modeling has long been dominated by Transformer-based architectures due to their strong performance across a wide range of tasks. However, their reliance on full self-attention [1] results in quadratic time and memory complexity with respect to sequence length, which limits scalability in long-context processing. This limitation has motivated a wave of recent efforts to revisit recurrent models or propose novel linear recurrent models such as state space models, linear attention methods [2–8].

By comparing these architectures, we observe a key difference between recurrent models and self-attention. Recurrent approaches compress the full sequence history into fixed-size and holistic representations, which can lead to degraded memory when modeling long sequences and limit precise information retrieval. In contrast, self-attention retains full-token access and thus does not suffer from the two problems, but at the cost of heavy computation. This motivates us to explore an intermediate design that partially compresses the sequence while still maintaining global access.

We propose a RAT layer, a simple yet effective temporal mixing method with a chunk-based design. It divides long sequences into chunks, applying recurrence within each chunk for local modeling and softmax-based attention across chunks for direct access to distant information (see Fig. 1a). Recurrence efficiently captures short-range dependencies while avoiding the memory degradation common

---

\*Correspondence to [xiuying.wei@epfl.ch](mailto:xiuying.wei@epfl.ch).



in long sequences, whereas attention over chunk-level representations enables long-range retrieval. By adjusting the chunk size  $L$ , RAT interpolates between attention (when  $L = 1$ ) and RNN (when  $L = T$ ).

To make RAT scalable and efficient, we further explore its positional encoding, parameter allocation, and efficient implementations that specifically address the causal masking problem in this chunk-based design. Moreover, we investigate a hybrid architecture that interleaves RAT with sliding-window attention [9–12], which focuses computation on local windows. As RAT suggests that overusing attention in local contexts underutilizes its strengths, and such dependencies can be handled more efficiently by lightweight recurrence, the two approaches can be complementary.

We demonstrate that RAT is both efficient and performant. For instance, with a chunk size of  $L = 16$ , the latency of a single temporal mixing block at position 4096 is up to  $9\times$  lower than that of standard attention. As shown in Table 1, the full model achieves up to  $10\times$  higher maximum throughput, and interleaving with local attention yields about  $4\times$  improvement. We pretrain models at 1.3B scale and compare their results on 1) zero-shot commonsense reasoning with short contexts, (2) long-context understanding on LongBench [13], and (3) supervised fine-tuning on long-context tasks. RAT with  $L = 16$  performs on par with full attention in most benchmarks and even outperforms it on several LongBench tasks. When interleaved with local attention, it achieves the best overall results across all variants while maintaining high efficiency. Our main contributions are as follows:

1. We propose the RAT layer, a novel intermediate architecture that bridges the efficiency of recurrence and the capacity of attention. It compresses only local context while preserving global access, enabling direct retrieval and avoiding the memory degradation caused by full sequence compression in long contexts.
2. RAT is simple, scalable, and efficient. It requires no custom CUDA kernels and is naturally compatible with existing multi-dimension parallelism schemes. We also introduce a hybrid variant by interleaving RAT with sliding-window attention, enabling efficient long-range modeling with strong local interactions.
3. We validate RAT through extensive experiments at the 1.3B scale across diverse tasks, including 7 short-context reasoning benchmarks, 11 long-context tasks, 4 supervised fine-tuning objectives, and 9 retrieval-heavy synthetic evaluations. RAT with  $L=16$  shows comparable performance to full attention with  $9\times$  faster single-layer decoding. Its hybrid variant with local attention yields the best overall results, along with a  $3 - 4\times$  maximum throughput boost—for instance, +1 accuracy on commonsense reasoning, +4 on code completion, +4 on a challenging QA task, and +1 on a difficult summarization task.

Table 1: Representative results for 1.3B models across pretraining, direct evaluation, and SFT. -SWA denotes interleaving with sliding-window attention (SWA) (window size 1024). Maximum throughput is measured by generating 1024 tokens given a prompt of 3072 tokens on a H100 GPU in GH200 system. See Sec. 4 for details.

Model	Throughput token/sec	Pretrain	Direct Evaluation				SFT	
		Val. PPL	CSR Avg. acc	SQA Avg. F1	Summ Avg. Rouge-L	Code Avg. EditSum	NQA <sup>1</sup> F1	QMSum Rouge-L
Attention	3052	7.61	56.9	18.2	<u>19.5</u>	<u>23.9</u>	61.3	<u>23.4</u>
RAT ( $L=16$ )	31170	7.67	56.7	<b>19.6</b>	<b>20.2</b>	17.4	60.8	23.3
Attention-SWA	4605	<u>7.61</u>	<u>57.1</u>	17.4	19.4	21.7	<b>63.3</b>	<u>23.4</u>
RAT ( $L=16$ ) -SWA	13582	<b>7.57</b>	<b>58.0</b>	<u>18.8</u>	<u>19.5</u>	<b>28.2</b>	<u>63.2</u>	<b>24.6</b>

## 2 Overall architecture

To motivate our design, we first examine how attention and recurrence compress contextual information at the token level, along with the equations that will be reused later. We then introduce RAT as an intermediate mechanism that inherits the respective advantages of both.

### 2.1 Attention: Full-Token Access

In softmax attention mechanisms, each token has access to all preceding tokens through a learned token-specific weighted aggregation:

$$\mathbf{y}_t = f(\mathbf{q}_t \mathbf{K}_{:,t}^\top) \mathbf{V}_{:,t} \quad (1)$$

$f(\cdot)$  denotes causal masking and the softmax function, and  $f(\mathbf{q}_t \mathbf{K}_{:,t}^\top)$  represents the attention weights used to aggregate  $\mathbf{V}_{:,t}$ . We adopt Python-style indexing in  $\mathbf{K}_{:,t}^\top, \mathbf{V}_{:,t}$  to emphasize that each query attends to all keys and values. This full-token access makes attention a dominant architecture in sequence modeling, but it suffers from high computational cost in both training and inference.

### 2.2 Recurrence: Full-Sequence Compression

Recurrent models maintain a summary of past information in a fixed-size representation, allowing each step to depend only on the previous state and the current input [14, 15]. To initiate the design of RAT, we adopt a simple and fast linear recurrence [16–18], which uses diagonal matrices and no nonlinearities to simplify the classic recurrence into an EMA-like gating mechanism:

$$\begin{aligned} \tilde{\mathbf{v}}_t &= \mathbf{g}_t \odot \tilde{\mathbf{v}}_{t-1} + (1 - \mathbf{g}_t) \odot \mathbf{v}_t, \\ \mathbf{y}_t &= \mathbf{z}_t \odot \tilde{\mathbf{v}}_t, \end{aligned} \quad (2)$$

where  $\mathbf{g}_t$  and  $\mathbf{z}_t \in \mathbb{R}^D$  denote the per-dimension forget and output gates, respectively, computed via linear projections of the input followed by a sigmoid activation. Here,  $D$  refers to the dimension of the model. This can be efficiently implemented using the parallel scan algorithm [18]. We take this minimal choice to highlight the core idea, but the recurrence in RAT is not limited to this certain form and can be extended to more advanced variants such as 2D recurrence or nonlinear RNNs. We leave this as future work.

The state-based formulation of recurrence yields low computational cost and efficient inference, and performs well on short sequences. However, compressing the entire sequence history into a fixed-size and holistic state, even with more expressive designs, can still suffer from memory degradation when the sequence length grows [19], and limits precise information retrieval, particularly in noisy contexts.

### 2.3 RAT: Chunk-Based Intermediate Design

To bridge the strong performance of attention enabled by full-token access with the efficiency of RNNs derived from full-sequence compression, we propose an intermediate design by reinterpreting the input as a sequence of shorter chunks. A recurrent module is applied within each chunk to model local dependencies, followed by cross-chunk attention to enable global interactions, as illustrated in Fig. 1a. This design mitigates the fixed-size representation limitation of RNNs and the inefficiency of attention.

Technically, we divide a sequence of length  $T$  into  $C$  chunks of length  $L$ , such that  $T = C \cdot L$ . A token originally at position  $t$  is re-indexed as  $(c, l)$ , where  $c$  denotes the chunk index and  $l$  the position within the chunk. Within each chunk, a forget gate  $\mathbf{g}_{c,l}$  is used to recurrently aggregate the value  $\mathbf{v}_{c,l}$  and key  $\mathbf{k}_{c,l}$  vectors, yielding updated representations  $\tilde{\mathbf{v}}_{c,l}$  and  $\tilde{\mathbf{k}}_{c,l}$ . For each query  $\mathbf{q}_{c,l}$ , we compute attention on the chunk-level key and value vectors, including  $\tilde{\mathbf{K}}_{:, -1}$  for all preceding chunks, and  $\tilde{\mathbf{k}}_{c,l}$  for the current chunk. The causal masking function  $f(\cdot)$  restricts attention to the chunks before it, followed by a softmax operation. Finally, an output gate is applied to produce the output:

$$\begin{aligned} \tilde{\mathbf{v}}_{c,l} &= \mathbf{g}_{c,l} \odot \tilde{\mathbf{v}}_{c,l-1} + (1 - \mathbf{g}_{c,l}) \odot \mathbf{v}_{c,l} && \text{(Intra-chunk RNN)} \\ \tilde{\mathbf{k}}_{c,l} &= \mathbf{g}_{c,l} \odot \tilde{\mathbf{k}}_{c,l-1} + (1 - \mathbf{g}_{c,l}) \odot \mathbf{k}_{c,l} && \text{(Intra-chunk RNN)} \\ \mathbf{y}_{c,l} &= f([\mathbf{q}_{c,l} \tilde{\mathbf{K}}_{:, -1}^\top; \mathbf{q}_{c,l} \tilde{\mathbf{k}}_{c,l}^\top]) [\tilde{\mathbf{V}}_{:, -1}; \tilde{\mathbf{v}}_{c,l}] && \text{(Inter-chunk attention)} \\ \mathbf{y}_{c,l} &= \mathbf{z}_{c,l} \odot \mathbf{y}_{c,l} \end{aligned} \quad (3)$$

The overall computation flow is illustrated in Fig. 1a. Thanks to the short length of each chunk, the recurrent module efficiently captures local dependencies without significant information loss. Cross-chunk attention then enables global access without compressing distant information. This design preserves the accuracy of softmax-based attention while reducing computation, as inter-chunk attention operates over shorter sequences with  $L$  as the FLOPs reduction ratio. We also experimented with a reversed variant by applying attention within chunks and recurrence across them, but found that standard RAT achieves better FLOPs utilization and overall performance (see Appendix C).

**Benefits of the chunk design** We position this as an **intermediate architecture** between RNNs and attention, and refer to it as RAT. By adjusting the chunk size  $L$ , RAT interpolates between their behaviors: when  $L=T$ , it reduces to a pure RNN; when  $L=1$ , it resembles full attention. This allows us to pursue the trade-off between attention and RNN with a single-layer design, and offers greater flexibility for hybrid modeling by using different chunk sizes to emulate varying behaviors. From a mechanistic perspective, unlike either classic or advanced recurrence (state space or linear attention models) that rely on fixed-size and holistic representations, our chunk-based structure enables memory capacity to scale with sequence length while maintaining a fixed FLOPs reduction ratio. Its partial compression with direct access to prior chunks ensures its superior performance on retrieval-heavy tasks.

### 3 Scalable and Efficient Modeling with RAT

#### 3.1 Design details

**Parameter allocation** We aim to control the parameters of RAT at  $4D^2$ , given  $D^2$  for the output projection,  $3D^2$  for the query, key, and value projections in attention, and an additional  $2D^2$  for the two gates in RNN. We explore lightweight alternatives by using low-rank projections for the gates  $g$  and  $z$ , or by sharing query and key projections across heads. Empirical results in Sec. 4.2 show that sharing the query  $q$  and key  $k$  slightly outperforms using low-rank gates. Notably, this design does not collapse into single-head attention, since the forget gate operates at the per-dimension level and produces distinct gated keys  $\tilde{k}$  for the inter-chunk attention.

**Positional encoding** We examine how to encode positional information in RAT, due to the presence of cross-chunk attention. Motivated by the fact that RNN captures positional information through its sequential structure, we find that applying positional encoding at the chunk level, rather than relying on original token positions, yields slightly better fidelity. This strategy also improves length generalization, as the number of positions requiring encoding (i.e., the number of chunks) is much smaller than the full sequence length. In our main experiments, we use RoPE [20] based on chunk indices for inter-chunk attention. In the length generalization study (see Subsec. C.2), we further explore NoPE [21], which yields the best overall generalization performance.

**Hybrid design with Local Attention** RAT is a hierarchical architecture, but not a hybrid model, as it applies the same strategy across all tokens, layers, and heads. It is compatible with various hybrid strategies and offers more flexibilities in hybrid modeling by varying the chunk size in different layers or heads. In particular, we explore interleaving RAT with sliding-window attention (SWA) [9–11], a widely adopted technique in recent models [22, 23, 5, 7]. We find that the two are highly complementary: while local attention methods allocate most computation within fixed windows, RAT reserves attention for global access and handles local modeling more efficiently. Interleaving them enables the model to efficiently and effectively capture both short-range and long-range dependencies.

#### 3.2 Efficiency

We discuss efficiency-related aspects of RAT, and show that our current implementation does not rely on custom CUDA or Triton kernels, yet achieves significant speed-ups in both training and generation in experiments. The pseudocode for training is provided in Listing 1, and the decoding algorithm is shown in Listing 2.

To begin, the FLOPs per token of RAT are  $\mathcal{O}(C \cdot D)$ , compared to  $\mathcal{O}(D)$  for RNN and  $\mathcal{O}(T \cdot D)$  for full attention, where  $C$  is the number of chunks,  $D$  the model dimension, and  $T$  the sequence length. Most components of RAT are simple and easy to implement, except that the chunk-based design introduces a non-trivial causal masking challenge during training, which we address below.

**Causal masking problem** In training, where tokens are processed in parallel, special care must be taken to apply causal masking in inter-chunk attention. First, a block-wise causal mask is required. Second, each token must also attend to its own chunk’s key and value, which should be gated up to its position. They vary across tokens due to causal masking, preventing efficient parallel computation. To address this, we adopt an online softmax formulation [24]: we separately compute  $f(\mathbf{q}_{c,l} \tilde{\mathbf{K}}_{:, -1}^\top) \tilde{\mathbf{V}}_{:, -1}$  and  $f(\mathbf{q}_{c,l} \tilde{\mathbf{k}}_{c,l}^\top) \tilde{\mathbf{v}}_{c,l}$ , and then combine the results by adjusting the softmax denominator. The first term can be implemented in parallel using existing attention frameworks, while the second is handled via a simple einsum.

**Practical implementation** For training, we implement intra-chunk recurrence in Eq. (3) using PyTorch’s *associative scan*, enabling forward and backward passes with  $\mathcal{O}(T)$  FLOPs. Compared to full-sequence recurrence, chunking reduces scan depth from  $\mathcal{O}(\log T)$  to  $\mathcal{O}(\log L)$  and thus improves parallelism. For inter-chunk attention, we use PyTorch’s *flex attention* to implement the first term above. It supports flash attention while providing flexibility features such as custom masks and returning the softmax denominator, that align well with our needs. For decoding, tokens are generated sequentially. Intra-chunk recurrence only requires single-step updates and can be implemented directly. For inter-chunk attention, standard implementations like *flash attention* [25] can be used without modification, as no complex causal masking is required at inference time.

**Parallelism** We think RAT is compatible with both tensor parallelism and context parallelism, which are commonly used for large model dimensions and long sequence lengths, respectively. Both the recurrence and cross-chunk attention in RAT are head-independent, making it easy to apply standard tensor parallelism by assigning different heads to different GPUs. For context parallelism, the intra-chunk recurrence is chunk-independent, allowing chunks to be distributed across GPUs. Since RAT stores much fewer number of chunk-level key/value vectors (e.g., 16× fewer than full attention), the cross-chunk attention may even avoid ring-style communication.

## 4 Experiments

In this section, we present the efficiency and large-scale evaluations of RAT, along with comparisons to other models. Additional discussions are provided in Appendix C.

### 4.1 Setup

For brevity, we summarize the setup for the 1.3B model with a 4K context window, which is used in most of our experiments. Full implementation details are available in Appendix A.

**Model** We adopt a Transformer architecture that interleaves a token mixing block with a hidden-state mixing block (FFN), each wrapped with residual connections and LayerNorm. We compare variants that use different token mixing modules, including RNN, attention, and RAT, as well as recent state space and linear attention models. In addition, we provide hybrid models that interleave RAT with sliding-window attention (window size 1024), such as Attention-SWA and RAT-SWA.

**Efficiency** We benchmark the latency of a single token mixing block, including input and output projections, on a single H100 GPU (GH200 system, 120GB), and also report the maximum throughput of the full model. We measure the time required to train on a full sequence or to generate a batch of tokens at specific positions. For fair comparison, we use *flash attention* for the attention baseline and *associative scan* for RNN. All models are compiled using *torch.compile* and evaluated in bfloat16 with *torch.cuda.amp*.

**Accuracy** We pretrain all 1.3B models on 100B tokens from FineWeb-Edu [26] using the same setup: a learning rate of 8.0e-4 decayed to 1.0e-6 (cosine schedule) and a global batch size of 2M tokens, following DeepSeek’s hyperparameter guidelines [27]. We directly evaluate the models on both short-context tasks—several classical commonsense reasoning benchmarks [28]—and long-context tasks, including 11 tasks from LongBench [13] covering QA, summarization, and code completion. Since LongBench includes instruction-heavy prompts that pretrained models often struggle with, we also include SFT-based evaluations. Specifically, we use NarrativeQA [29] (two modes), QMSum [30], and WikiSum [31] to test long-context understanding across a range of input

lengths. To assess retrieval capabilities, we include the Ruler benchmark [32], which comprises nine synthetic needle-in-haystack tasks with varying configurations. A single round of lightweight fine-tuning is applied to adapt models to specific prompts.

## 4.2 Analyses of RAT

Figure 2: **Latency of the temporal mixing block** (including linear projections) with a model dimension of 2048. (a): full-sequence latency with 200K tokens; (b): generation of 512 tokens at specified positions. We adopt *flash attention* for Attention.

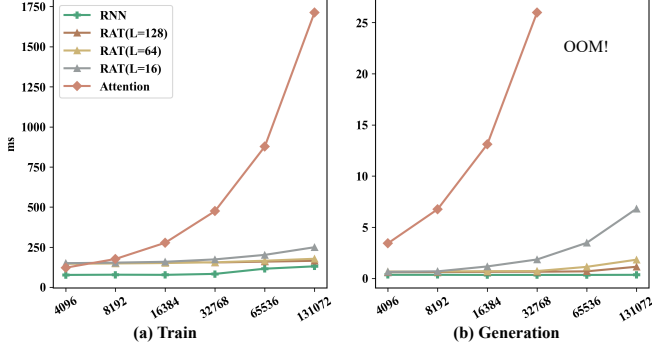


Table 2: **Maximum throughput of full models** (tokens/sec), measured by generating 1024 tokens from a 3072-token prompt. By reducing the KV cache memory and boosting speed, we achieve 10× maximum throughput compared to *flash attention*, and even more on 13B models, as attention suffers from poor GPU utilization at larger scale.

Model	1.3B	7B	13B
RAT(L=16)	31170	10103	5749
Attention	3152	983	534
Ratio	10.2×	10.3×	10.8×

**Efficiency study** Fig. 2 and Table 2 present the efficiency comparison, with additional results provided in Appendix B. For training, on the strong H100 GPU, when the sequence length is short (e.g., 4096), RAT is slightly slower than attention due to underutilized GPU parallelism in the *flex attention* (with only 256 chunks) and the overhead introduced by *associative scan*. We expect these can be improved through further kernel-level optimizations. As the sequence length increases, RAT becomes increasingly efficient: for  $L = 16$ , we observe approximately 2× speedup at 16K, 3× at 32K, 4× at 64K, and 7× at 100K tokens. For generation, RAT(L=16) achieves a 9× speedup at position 4K and around 10× for longer sequences. It also reduces KV cache usage, making it significantly less prone to out-of-memory (OOM) errors and enabling much higher maximum throughput.

**Ablation study** We conduct the ablation study on a 200M-parameter model trained on the book dataset. Allocating more parameters to the intra-chunk RNN gates yields significantly better performance than assigning them to the inter-chunk attention query and key projections, improving the perplexity by 0.4–0.5. Further replacing the original RoPE with a cross-chunk variant, where positions are indexed by chunk index, brings additional improvement, especially at long sequence lengths, with a 0.3 drop in PPL observed.

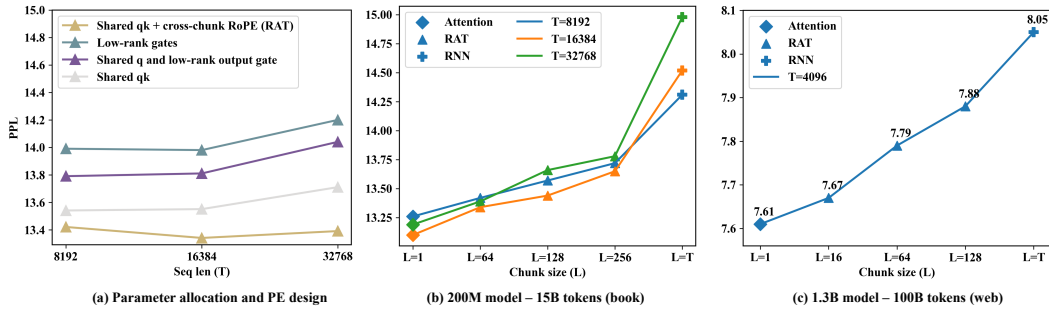


Figure 3: (a) Ablation study on RAT(L=64). (b) and (c) show pretraining results on 200M and 1.3B models, respectively. RAT lies between RNN and attention in terms of pretraining perplexity.

**Pretraining** In Fig. 3(b) and (c), we begin our study by examining pretraining perplexity as a foundational measure of architectural performance, demonstrating that RAT falls between attention and

RNN. In (b), using a 200M model, we observe that increasing the chunk size leads to higher perplexity while reducing FLOPs. Viewing attention as  $L = 1$  and RNN as  $L = T$ , we observe perplexities of 13.26 for attention, 13.42 for RAT( $L=64$ ), 13.72 for RAT( $L=256$ ), and 14.31 for RNN. Interestingly, increasing the training context from  $T = 8192$  to  $T = 32768$  leads to a sharp rise in perplexity for RNN, while both attention and RAT remain stable, demonstrating the pitfalls of full-sequence compression. We then scale up to a 1.3B model trained on web data, which primarily consists of short sequences (often under 1K tokens) concatenated with separator tokens to construct 4K-length contexts. In this regime, we find that RAT( $L=16$ ) gives the comparable performance to attention, and again RAT with different chunk sizes exhibits behavior intermediate between attention and RNN.

### 4.3 Large-scale evaluation and comparisons

In this section, we present direct evaluation and SFT results of our trained 1.3B models. We mainly compare RAT( $L=16$ ) with its two extremes: RNN and attention. Additionally, we include results from recent state space and linear attention models [5], which are trained under the same settings (model size, sequence length, and dataset) as ours. We report the value/slot sizes, which indicates the size of memory slots and FLOPs, based on sequence length  $T$ , model dimension  $D$ , and number of layers  $N$ . Note that state space and linear attention models use fixed-size memory and expand the classic recurrence state, while RAT scales its memory capacity with the sequence length.

**Commonsense reasoning** In Table 3, the performance gap (within two points on average) between RNN and attention is small on these short commonsense reasoning tasks, indicating that RNN can be surprisingly competitive in short-context settings. RAT( $L=16$ ) consistently outperforms RNN on most tasks and surpasses other recent models on 4 out of 7 benchmarks, with only at most  $20ND$  memory slots. We also observe that some binary-choice tasks (e.g., BoolQ, WinoGrande) show inconsistent results under small-scale pretraining. For instance, attention struggles on BoolQ, while RAT underperforms on WinoGrande. Interestingly, the hybrid variant RAT( $L=16$ )-SWA, which interleaves RAT with SWA, achieves the best overall accuracy across almost all tasks. This suggests a complementary architecture: using SWA for strong local attention and RAT for long-range dependencies can bring us a model that is not only more efficient but also more accurate than its dense counterpart.

Table 3: We evaluate our models with model dimension  $D = 2048$  and number of layers  $N = 24$  on seven commonsense reasoning tasks using *lm-evaluation-harness* [28]. Since all tasks (except BoolQ, which has only 13 sequences  $> 300$  tokens) have sequences  $\leq 300$  tokens, we set  $T = 300$ . Results marked with \* are from a recent study [5] trained on the same setting as ours. For SWA, slot sizes remain  $150ND$  due to the short context.

Model	Value/Slot size $T=300$	ARC-C acc/acc_n	ARC-E acc/acc_n	HellaSwag acc/acc_n	LAMBADA acc	PIQA acc/acc_n	WinoGrande acc	BoolQ acc
RNN	$ND$	35.15/38.57	70.66/66.46	42.43/55.95	39.74	71.49/72.69	53.99	62.54
Mamba*	$64ND$	-/35.40	69.52/-	-/52.91	-/43.98	71.32/-	52.95	61.13
Mamba2*	$256ND$	-/37.88	72.47/-	-/55.67	-/45.66	71.87/-	55.24	60.13
DeltaNet*	$128ND$	-/35.66	68.47/-	-/50.93	-/42.46	70.72/-	53.35	55.29
GatedDeltaNet*	$288ND$	-/38.39	71.21/-	-/55.76	-/46.65	72.25/-	57.45	60.24
Attention	$300ND$	35.67/37.71	71.25/66.67	<b>44.16/57.44</b>	<b>47.84</b>	<b>73.29/72.91</b>	<b>57.70</b>	58.23
RAT( $L=16$ )	$\sim 20ND$	<b>36.35/39.33</b>	<b>72.64/67.80</b>	43.27/56.44	44.40	72.03/72.69	53.20	<b>63.30</b>
GatedDeltaNet-SWA*	$288N/2D - 300N/2D$	-/40.10	71.75/-	-/56.53	47.73	72.57/-	<b>58.4</b>	63.21
Attention-SWA	$300N/2D - 300N/2D$	35.24/37.20	71.97/66.20	44.36/57.09	47.97	72.25/72.74	56.91	61.25
RAT( $L=16$ )-SWA	$\sim 20N/2D - 300N/2D$	<b>37.20/40.78</b>	<b>72.56/68.22</b>	<b>44.33/57.85</b>	<b>49.33</b>	<b>73.29/73.94</b>	56.91	<b>63.21</b>

**LongBench** In Table 4, we present results on 11 long-context tasks from LongBench. Since LongBench includes instruction-heavy prompts across diverse domains, it’s natural that no single model dominates all tasks. Evaluating purely pretrained models on such instruction-based datasets can be very challenging. Therefore, we focus on general performance trends, especially average scores by task category. As shown in the table, RAT( $L=16$ ) and its hybrid variant RAT( $L=16$ )-SWA achieve top performance in many groups, such as question answering and summarization. This is noteworthy, given that RAT( $L=16$ ) slightly lags behind attention in pretraining perplexity and underperforms in short-context commonsense reasoning. We hypothesize that its advantage on LongBench stems from structural adaptation to very long sequences—for instance, achieving 24.9 on GovReport (3-1) (vs. 18.6 for the attention baseline) and 16.7 on HotpotQA (2-1) (vs. 13.4). Second, unlike the small gap ( $\sim 2$  points) between RNN and attention on short-context tasks, the difference becomes much larger on LongBench, further demonstrating the problem of full-sequence compression. We also notice that

Table 4: Evaluation results on LongBench with  $T = 4096$ ,  $D = 2048$ , and  $N = 24$ . NQA: NarrativeQA, MQA: MultiFieldQA-en, HQA: HotpotQA, WQA: 2WikiMultihopQA, MSQ: Musique, GR: GovReport, MN: MultiNews, TQA: TriviaQA, RBP: RepoBench-P. Metrics: F1 for QA tasks, Rouge-L for summarization, and EditSum for code tasks. Results marked with \* are from a recent study [5] trained under the same settings as ours. Note that they use local attention with a window size of 2048, while we use 1024.

Model	Value/Slot size $T = 4096$	Single-Document QA				Multi-Document QA				Summarization				Code Completion		
		NQA	Qasper	MQA	Avg.	HQA	WQA	MSQ	Avg.	GR	QMSum	MN	Avg.	LCC	RBP	Avg.
RNN	$ND$	11.7	8.8	19.5	13.3	9.1	15.1	5.4	9.9	16.9	16.8	16.4	16.7	14.0	17.6	15.8
Mamba2*	$256ND$	11.1	11.3	18.6	13.7	11.8	15.1	<b>6.7</b>	11.2	6.7	14.5	7.4	9.5	17.9	20.6	19.3
DeltaNet*	$128ND$	12.9	10.8	21.5	15.1	10.9	13.2	5.1	9.7	6.5	13.5	7.2	9.1	17.6	20.3	19.0
GatedDeltaNet*	$288ND$	14.1	14.0	23.3	17.1	13.7	14.4	5.8	11.3	7.5	16.4	7.9	10.6	18.7	22.1	20.4
Attention	$4096ND$	12.3	14.0	28.2	18.2	13.4	17.7	4.9	12.0	18.6	<b>18.9</b>	<b>21.0</b>	19.5	<b>21.3</b>	<b>26.5</b>	<b>23.9</b>
RAT(L=64)	$64ND$	13.9	13.0	27.0	18.0	14.9	16.3	4.3	11.8	18.9	17.7	19.9	18.8	16.2	19.7	18.0
RAT(L=16)	$256ND$	<b>14.5</b>	<b>16.1</b>	<b>28.3</b>	<b>19.6</b>	<b>16.7</b>	<b>18.9</b>	6.3	<b>14.0</b>	<b>24.9</b>	17.5	18.3	<b>20.2</b>	14.2	20.6	17.4
GatedDeltaNet-SWA*	$288N/2D - 2048N/2D$	<b>14.5</b>	12.3	26.6	17.8	12.6	<b>23.6</b>	6.1	<b>14.1</b>	9.1	16.1	12.8	12.7	15.5	19.2	17.4
Attention-SWA	$4096N/2D - 1024N/2D$	13.1	14.6	24.5	17.4	13.7	19.0	6.1	12.9	19.4	17.3	<b>21.4</b>	19.4	18.7	24.6	21.7
RAT(L=16)-SWA	$256N/2D - 1024N/2D$	12.7	<b>15.6</b>	<b>28.2</b>	<b>18.8</b>	<b>14.2</b>	18.1	<b>7.4</b>	13.2	<b>20.1</b>	<b>18.6</b>	19.8	<b>19.5</b>	<b>26.3</b>	<b>30.1</b>	<b>28.2</b>

RAT(L=16) performs less favorably on code completion. However, its hybrid variant significantly improves performance in this setting, outperforming the second-best model by about four points.

**Supervised Fine-tuning** Since LongBench tasks are instruction-based and pretrained-only models often struggle to follow specific prompts, we further assess the performance of SFT on some long-context QA and summarization tasks, as shown in Table 5. For NarrativeQA, where passages are extremely long and may not contain the answer within the truncated 4K-token context, we evaluate two settings: (1) summary-only, which uses only the passage summary, and (2) summary plus passage, which concatenates the summary with the full passage. In both cases, RAT(L=16)-SWA delivers strong performance while remaining efficient. Although both the summary and passage contain useful information, we observe that models, particularly the attention-based ones, perform worse in the second setting, with F1 dropping to 33. We hypothesize that in this setup, attention may be more easily distracted due to the absence of structural bias, which can lead to flattened attention score distributions [33]. In contrast, models based on RAT appear more robust, likely due to their chunk-wise structure. For summarization tasks, RNN performs better than in QA, and RAT(L=16)-SWA achieves the best result on QMSum, surpassing the next-best model by approximately 1 Rouge-L point.

Table 5: **Left:** Average and 95th percentile of context lengths of datasets with the LLaMA2 tokenizer. **Right:** SFT performance on long-context datasets with  $T = 4096$ ,  $D = 2048$ , and  $N = 24$ . F1 is used for QA tasks, and Rouge-L is used for summarization tasks. NarrativeQA<sup>1</sup>: only the summary of a passage is provided. NarrativeQA<sup>2</sup>: the summary plus the full passage is provided; the passage typically contains much irrelevant information.

Task	Avg.	95th pctl.	Model	Value/Slot size	NarrativeQA <sup>1</sup>	NarrativeQA <sup>2</sup>	QMSum	WikiSum
NarrativeQA <sup>1</sup>	838	1296	RNN	$ND$	30.5	27.4	23.2	34.3
NarrativeQA <sup>2</sup>	97k	254k	RAT(L=16)	$256ND$	60.8	43.5	23.3	36.6
QMSum	16k	29k	Attention	$4096ND$	61.3	33.0	23.4	36.8
WikiSum	1828	3473	Attention-SWA	$4096N/2D - 1024N/2D$	<b>63.3</b>	39.6	23.4	36.7
			RAT(L=16)-SWA	$256N/2D - 1024N/2D$	63.2	<b>43.7</b>	<b>24.6</b>	36.7

Table 6: **Retrieval ability:** Accuracy performance with exact match scoring on the Needle-in-Haystack tasks with different configurations from the RULER benchmark [32]. We use  $T = 4096$ ,  $D = 2048$ , and  $N = 24$ .

Model	Value/Slot size	single_1	single_2	single_3	multikey_1	multikey_2	multikey_3	multiquery	multivalue
RNN	$ND$	99.4	99.8	0.0	2.2	0.0	0.0	5.8	5.7
RAT(L=64)	$64ND$	100.0	99.8	55.6	96.4	62.2	1.0	86.3	89.1
RAT(L=16)	$256ND$	99.6	100.0	94.6	99.6	99.6	82.6	91.2	94.8
Attention	$4096ND$	100.0	100.0	100.0	99.6	99.6	95.2	98.6	99.1

**Retrieval ability** In Table 6, we evaluate the three models on challenging synthetic needle-in-haystack tasks that test retrieval ability (see Subsec. C.3 for task descriptions). It can be seen that attention consistently performs well due to its full-token access. RNN handles simpler tasks like `single_1` and `single_2` reasonably well, but its performance drops on harder settings. RAT(L=16) matches attention closely on most tasks but struggles with UUID ones (`single_3`, `multikey_3`) due to their difficulty and evaluation metric as exact match scoring. Meanwhile, RAT(L=64) falls



between RNNs and RAT ( $L=16$ ), as expected given its partial access to long-range context. These results align with the model structures: attention sees all tokens directly, recurrence compresses all history into a single state, and RAT blends both, preserving chunk-level access while reducing FLOPs.

## 5 Related work

**State space and linear attention models** Recurrent neural networks (RNNs) have long been used for sequential modeling [34–36]. Recent state space models [37, 18, 2, 7, 8] extend recurrence by expanding hidden states from vectors to matrices for higher accuracy, removing non-linearity and using structured operations (e.g., diagonal matrices) to enable parallel computation [18]. Per-head gating connects these models [3] to linear attention [4, 38, 39, 8, 40, 5] and shows the duality between linear recurrence and linear attention. Unlike this duality perspective, we take an intermediate view between per-dimension-gated RNNs and softmax-based attention, without enforcing strict linearity. Linear recurrence in RAT is intended primarily for training efficiency, rather than imposed as a design constraint.

Despite state expansion, these models inherit the fixed-size representation limitation of classic RNNs, leading to degraded memory on long sequences. A concurrent work [41] proposes addressing this by growing the memory slots logarithmically. We similarly target the fixed-size memory problem, but use softmax-based attention to access distant tokens. Hybrid strategies combining state space models and attention are also popular. While RAT is not a hybrid with the same computation graph for all tokens and all layers, it is orthogonal to such designs and provides more flexibility, such as using different chunk sizes for different layers and heads, which we leave for future work.

**Softmax-based attention** Attention mechanisms suffer from slow computation due to their full-token access. Earlier works have explored local attention with chunking, combined with recurrence or sparse mechanisms to access earlier context [9, 10, 42–44]. For example, Ma et al. [42] gates query/key vectors before local attention, while Hua et al. [10] adds the outputs of local attention to cross-chunk linear attention. In our work, we instead leverage attention’s strength in directly accessing distant tokens with lightweight recurrence for local contexts, and hierarchically organize their outputs. As shown in Sec. C.1, RAT utilizes FLOPs more effectively than local attention. We also regard RAT and local attention as structurally complementary. Although we experimented with interleaving them in this work, we leave the combination with more advanced local attention variants in future research.

RAT can be viewed as an attention mechanism with resolution, akin to how humans process information: short-term inputs are integrated into coherent representations, while long-term events are stored as memory anchors for selective retrieval. Compared to dilated attention [9], our simple recurrence enables global perception, and the chunk-level attention has high training parallelism and reduced cache memory (see Sec. C.1 for more). Finally, a recent work [45] also aggregates the key and value vectors and applies softmax-based attention over them. However, it compresses the full-sequence vectors into a 2D memory matrix, unlike our chunk-based design, which enables flexible memory slots.

## 6 Conclusion

This paper proposes the RAT structure, an intermediate architecture between RNN and attention. It segments sequences into chunks, applies RNN within each chunk to capture local dependencies, and employs attention across chunks to model long-range dependencies. We detail its architectural design and investigate its combination with the sliding-window attention mechanism. Experimental results across various settings demonstrate the efficiency and accuracy benefits of RAT, highlighting its potential for future language model development.

**Limitations.** Due to resource constraints and the exploratory nature of this work, our experiments are limited to models with up to 1.3B parameters. We have not yet scaled RAT to larger language models such as 7B or 14B to confirm our results hold at that scale. Additionally, we did not adopt supervised fine-tuning techniques commonly used in current industry practices, which typically involve substantial data resources and many engineering details. Instead, we followed a more classical approach based on train-test splits to evaluate performance, as our focus lies primarily on architectural design during pretraining. Lastly, RAT may still face length generalization issues from positional encoding, similar to attention. But as shown in Subsec. C.2, this can be significantly reduced by shorter inter-chunk attention spans, and we also explore the use of NoPE.

## Acknowledgments and Disclosure of Funding

We sincerely thank the RCP and the SCITAS team at EPFL for GPU support. We also thank the Swiss AI Initiative and the Swiss National Supercomputing Centre (CSCS) for supporting this work through grants under project IDs a06 and a10. We thank Skander Moalla, Anja Surina, and Lars Quaadvlieg for helpful discussion on SFT tasks. We extend our appreciation to Karin Getaz for administrative support.

## References

- [1] A Vaswani. Attention is all you need. *Advances in Neural Information Processing Systems*, 2017.
- [2] Albert Gu and Tri Dao. Mamba: Linear-time sequence modeling with selective state spaces. *arXiv preprint arXiv:2312.00752*, 2023.
- [3] Tri Dao and Albert Gu. Transformers are ssms: Generalized models and efficient algorithms through structured state space duality. *arXiv preprint arXiv:2405.21060*, 2024.
- [4] Angelos Katharopoulos, Apoorv Vyas, Nikolaos Pappas, and François Fleuret. Transformers are rnns: Fast autoregressive transformers with linear attention. In *International conference on machine learning*, pages 5156–5165. PMLR, 2020.
- [5] Songlin Yang, Jan Kautz, and Ali Hatamizadeh. Gated delta networks: Improving mamba2 with delta rule. *arXiv preprint arXiv:2412.06464*, 2024.
- [6] Maximilian Beck, Korbinian Pöppel, Markus Spanring, Andreas Auer, Oleksandra Prudnikova, Michael Kopp, Günter Klambauer, Johannes Brandstetter, and Sepp Hochreiter. xlstm: Extended long short-term memory. *arXiv preprint arXiv:2405.04517*, 2024.
- [7] Soham De, Samuel L Smith, Anushan Fernando, Aleksandar Botev, George Cristian-Muraru, Albert Gu, Ruba Haroun, Leonard Berrada, Yutian Chen, Srivatsan Srinivasan, et al. Griffin: Mixing gated linear recurrences with local attention for efficient language models. *arXiv preprint arXiv:2402.19427*, 2024.
- [8] Antonio Orvieto, Samuel L Smith, Albert Gu, Anushan Fernando, Caglar Gulcehre, Razvan Pascanu, and Soham De. Resurrecting recurrent neural networks for long sequences. In *International Conference on Machine Learning*, pages 26670–26698. PMLR, 2023.
- [9] Iz Beltagy, Matthew E Peters, and Arman Cohan. Longformer: The long-document transformer. *arXiv preprint arXiv:2004.05150*, 2020.
- [10] Weizhe Hua, Zihang Dai, Hanxiao Liu, and Quoc Le. Transformer quality in linear time. In *International conference on machine learning*, pages 9099–9117. PMLR, 2022.
- [11] Zihang Dai, Zhilin Yang, Yiming Yang, Jaime Carbonell, Quoc V Le, and Ruslan Salakhutdinov. Transformer-xl: Attentive language models beyond a fixed-length context. *arXiv preprint arXiv:1901.02860*, 2019.
- [12] DeLesley Hutchins, Imanol Schlag, Yuhuai Wu, Ethan Dyer, and Behnam Neyshabur. Block-recurrent transformers. *Advances in neural information processing systems*, 35: 33248–33261, 2022.
- [13] Yushi Bai, Xin Lv, Jiajie Zhang, Hongchang Lyu, Jiankai Tang, Zhidian Huang, Zhengxiao Du, Xiao Liu, Aohan Zeng, Lei Hou, et al. Longbench: A bilingual, multitask benchmark for long context understanding. *arXiv preprint arXiv:2308.14508*, 2023.
- [14] Junyoung Chung, Caglar Gulcehre, KyungHyun Cho, and Yoshua Bengio. Empirical evaluation of gated recurrent neural networks on sequence modeling. *arXiv preprint arXiv:1412.3555*, 2014.
- [15] S Hochreiter. Long short-term memory. *Neural Computation MIT-Press*, 1997.
- [16] Leo Feng, Frederick Tung, Mohamed Osama Ahmed, Yoshua Bengio, and Hossein Hajimirsadeghi. Were rnns all we needed? *arXiv preprint arXiv:2410.01201*, 2024.

- [17] Eric Martin and Chris Cundy. Parallelizing linear recurrent neural nets over sequence length. *arXiv preprint arXiv:1709.04057*, 2017.
- [18] Jimmy TH Smith, Andrew Warrington, and Scott W Linderman. Simplified state space layers for sequence modeling. *arXiv preprint arXiv:2208.04933*, 2022.
- [19] Razvan Pascanu, Tomas Mikolov, and Yoshua Bengio. On the difficulty of training recurrent neural networks. In *International conference on machine learning*, pages 1310–1318. Pmlr, 2013.
- [20] Jianlin Su, Murtadha Ahmed, Yu Lu, Shengfeng Pan, Wen Bo, and Yunfeng Liu. Roformer: Enhanced transformer with rotary position embedding. *Neurocomputing*, 568:127063, 2024.
- [21] Amirhossein Kazemnejad, Inkit Padhi, Karthikeyan Natesan Ramamurthy, Payel Das, and Siva Reddy. The impact of positional encoding on length generalization in transformers. *Advances in Neural Information Processing Systems*, 36:24892–24928, 2023.
- [22] Team Cohere, Arash Ahmadian, Marwan Ahmed, Jay Alammari, Milad Alizadeh, Yazeed Alnumay, Sophia Althammer, Arkady Arkhangorodsky, Viraat Aryabumi, Dennis Aumiller, et al. Command a: An enterprise-ready large language model. *arXiv preprint arXiv:2504.00698*, 2025.
- [23] Liliang Ren, Yang Liu, Yadong Lu, Yelong Shen, Chen Liang, and Weizhu Chen. Samba: Simple hybrid state space models for efficient unlimited context language modeling. *arXiv preprint arXiv:2406.07522*, 2024.
- [24] Maxim Milakov and Natalia Gimelshein. Online normalizer calculation for softmax. *arXiv preprint arXiv:1805.02867*, 2018.
- [25] Tri Dao, Dan Fu, Stefano Ermon, Atri Rudra, and Christopher Ré. Flashattention: Fast and memory-efficient exact attention with io-awareness. *Advances in neural information processing systems*, 35:16344–16359, 2022.
- [26] Guilherme Penedo, Hynek Kydlíček, Anton Lozhkov, Margaret Mitchell, Colin A Raffel, Leandro Von Werra, Thomas Wolf, et al. The fineweb datasets: Decanting the web for the finest text data at scale. *Advances in Neural Information Processing Systems*, 37:30811–30849, 2024.
- [27] Xiao Bi, Deli Chen, Guanting Chen, Shanhuang Chen, Damai Dai, Chengqi Deng, Honghui Ding, Kai Dong, Qiusi Du, Zhe Fu, et al. Deepseek llm: Scaling open-source language models with longtermism. *arXiv preprint arXiv:2401.02954*, 2024.
- [28] Leo Gao, Jonathan Tow, Baber Abbasi, Stella Biderman, Sid Black, Anthony DiPofi, Charles Foster, Laurence Golding, Jeffrey Hsu, Alain Le Noac’h, Haonan Li, Kyle McDonell, Niklas Muennighoff, Chris Ociepa, Jason Phang, Laria Reynolds, Hailey Schoelkopf, Aviya Skowron, Lintang Sutawika, Eric Tang, Anish Thite, Ben Wang, Kevin Wang, and Andy Zou. The language model evaluation harness, 07 2024. URL <https://zenodo.org/records/12608602>.
- [29] Tomáš Kočiský, Jonathan Schwarz, Phil Blunsom, Chris Dyer, Karl Moritz Hermann, Gábor Melis, and Edward Grefenstette. The narrativeqa reading comprehension challenge. *Transactions of the Association for Computational Linguistics*, 6:317–328, 2018.
- [30] Ming Zhong, Da Yin, Tao Yu, Ahmad Zaidi, Mutethia Mutuma, Rahul Jha, Ahmed Hassan Awadallah, Asli Celikyilmaz, Yang Liu, Xipeng Qiu, et al. Qmsum: A new benchmark for query-based multi-domain meeting summarization. *arXiv preprint arXiv:2104.05938*, 2021.
- [31] Nachshon Cohen, Oren Kalinsky, Yftah Ziser, and Alessandro Moschitti. Wikisum: Coherent summarization dataset for efficient human-evaluation. In *Proceedings of the 59th Annual Meeting of the Association for Computational Linguistics and the 11th International Joint Conference on Natural Language Processing (Volume 2: Short Papers)*, pages 212–219, 2021.
- [32] Cheng-Ping Hsieh, Simeng Sun, Samuel Kriman, Shantanu Acharya, Dima Rekesch, Fei Jia, Yang Zhang, and Boris Ginsburg. Ruler: What’s the real context size of your long-context language models? *arXiv preprint arXiv:2404.06654*, 2024.
- [33] Ken M Nakanishi. Scalable-softmax is superior for attention. *arXiv preprint arXiv:2501.19399*, 2025.

- [34] Jeffrey L Elman. Finding structure in time. *Cognitive science*, 14(2):179–211, 1990.
- [35] Hava T Siegelmann and Eduardo D Sontag. On the computational power of neural nets. In *Proceedings of the fifth annual workshop on Computational learning theory*, pages 440–449, 1992.
- [36] Yoshua Bengio, Patrice Simard, and Paolo Frasconi. Learning long-term dependencies with gradient descent is difficult. *IEEE transactions on neural networks*, 5(2):157–166, 1994.
- [37] Albert Gu, Karan Goel, and Christopher Ré. Efficiently modeling long sequences with structured state spaces. *arXiv preprint arXiv:2111.00396*, 2021.
- [38] Yutao Sun, Li Dong, Shaohan Huang, Shuming Ma, Yuqing Xia, Jilong Xue, Jianyong Wang, and Furu Wei. Retentive network: A successor to transformer for large language models. *arXiv preprint arXiv:2307.08621*, 2023.
- [39] Bo Peng, Eric Alcaide, Quentin Anthony, Alon Albalak, Samuel Arcadinho, Stella Biderman, Huanqi Cao, Xin Cheng, Michael Chung, Matteo Grella, et al. RwkV: Reinventing rnns for the transformer era. *arXiv preprint arXiv:2305.13048*, 2023.
- [40] Songlin Yang, Bailin Wang, Yu Zhang, Yikang Shen, and Yoon Kim. Parallelizing linear transformers with the delta rule over sequence length. *arXiv preprint arXiv:2406.06484*, 2024.
- [41] Han Guo, Songlin Yang, Tarushii Goel, Eric P Xing, Tri Dao, and Yoon Kim. Log-linear attention. *arXiv preprint arXiv:2506.04761*, 2025.
- [42] Xuezhe Ma, Chunting Zhou, Xiang Kong, Junxian He, Liangke Gui, Graham Neubig, Jonathan May, and Luke Zettlemoyer. Mega: moving average equipped gated attention. *arXiv preprint arXiv:2209.10655*, 2022.
- [43] Xuezhe Ma, Xiaomeng Yang, Wenhan Xiong, Beidi Chen, Lili Yu, Hao Zhang, Jonathan May, Luke Zettlemoyer, Omer Levy, and Chunting Zhou. Megalodon: Efficient llm pretraining and inference with unlimited context length. *Advances in Neural Information Processing Systems*, 37:71831–71854, 2024.
- [44] Amirkeivan Mohtashami and Martin Jaggi. Landmark attention: Random-access infinite context length for transformers. *arXiv preprint arXiv:2305.16300*, 2023.
- [45] Yu Zhang, Songlin Yang, Rui-Jie Zhu, Yue Zhang, Leyang Cui, Yiqiao Wang, Bolun Wang, Freda Shi, Bailin Wang, Wei Bi, et al. Gated slot attention for efficient linear-time sequence modeling. *Advances in Neural Information Processing Systems*, 37:116870–116898, 2024.
- [46] Jack W Rae, Anna Potapenko, Siddhant M Jayakumar, Chloe Hillier, and Timothy P Lillicrap. Compressive transformers for long-range sequence modelling. *arXiv preprint*, 2019. URL <https://arxiv.org/abs/1911.05507>.
- [47] Yonatan Bisk, Rowan Zellers, Jianfeng Gao, Yejin Choi, et al. Piqa: Reasoning about physical commonsense in natural language. In *Proceedings of the AAAI conference on artificial intelligence*, volume 34, pages 7432–7439, 2020.
- [48] Peter Clark, Isaac Cowhey, Oren Etzioni, Tushar Khot, Ashish Sabharwal, Carissa Schoenick, and Oyvind Tafjord. Think you have solved question answering? try arc, the ai2 reasoning challenge. *arXiv:1803.05457v1*, 2018.
- [49] Rowan Zellers, Ari Holtzman, Yonatan Bisk, Ali Farhadi, and Yejin Choi. Hellaswag: Can a machine really finish your sentence? *arXiv preprint arXiv:1905.07830*, 2019.
- [50] Biao Zhang and Rico Sennrich. Root mean square layer normalization. *Advances in Neural Information Processing Systems*, 32, 2019.
- [51] Bowen Peng, Jeffrey Quesnelle, Honglu Fan, and Enrico Shippole. Yarn: Efficient context window extension of large language models. *arXiv preprint arXiv:2309.00071*, 2023.
- [52] bloc97. NTK-Aware Scaled RoPE allows LLaMA models to have extended (8k+) context size without any fine-tuning and minimal perplexity degradation, 2023.
- [53] Jie Wang, Tao Ji, Yuanbin Wu, Hang Yan, Tao Gui, Qi Zhang, Xuanjing Huang, and Xiaoling Wang. Length generalization of causal transformers without position encoding. *arXiv preprint arXiv:2404.12224*, 2024.

## A Implementation details

### A.1 Algorithm

We provide the pseudocode for the training and prefilling modes of RAT in Listing 1, and the pseudocode for the generation mode in Listing 2.

```
1 def merge_last_token_stable
  (inter_out, intra_out, inter_lse, intra_lse):
2   # Merge previous chunk's output and current chunk's output safely
3   # by adjusting the base of the exponential in softmax
4   max_lse = maximum(inter_lse, intra_lse)
5   inter_lse_exp = exp(inter_lse - max_lse)
6   intra_lse_exp = exp(intra_lse - max_lse)
7   denom = intra_lse_exp + inter_lse_exp
8   intra_adjust = (intra_lse_exp / denom).unsqueeze(-1)
9   inter_adjust = (inter_lse_exp / denom).unsqueeze(-1)
10  return inter_out * inter_adjust + intra_out * intra_adjust
11
12
13 def train_or_prefill
  (z, g, q, k, v, num_chunk, chunk_size, num_head, softmax_scale):
14   """
15   Args:
16   z: (B, T, D), output gate after sigmoid function
17   g: (B, T, D), forget gate after sigmoid function
18   v: (B, T, D), value vectors in attention
19   q, k: (B, T, D), shared query and key vectors in attention
20   Returns:
21   out: (B, T, D)
22   """
23   bs, seq_len, d_model = shape(z)
24   k, v = [
25     rearrange(m, "b (c l) d -> b c l d", c=num_chunk) for m in (k, v)]
26
27   # Intra-chunk RNN: apply associative scan along the "l" dimension
28   intra_v = ascan(g, (1.0 - g) * v)
29   intra_k = ascan(g, (1.0 - g) * k)
30
31   # Rearrange for multi-head attention
32   intra_v = rearrange(intra_v, "b c l (a p) -> b a (c l) p", a=num_head)
33   intra_k = rearrange(intra_k, "b c l (a p) -> b a (c l) p", a=num_head)
34   q = rearrange(q, "b t (a p) -> b a t p", a=num_head)
35
36   # Apply inter-chunk RoPE
37   q, intra_k = apply_rope(q, intra_k)
38
39   # Extract chunk's end representation for inter-chunk attention
40   chunk_intra_k = intra_k[..., chunk_size - 1::chunk_size, :]
41   chunk_intra_v = intra_v[..., chunk_size - 1::chunk_size, :]
42
43   # Inter-chunk attention using flex_attention
44   # with chunk-level causal mask and returning log-sum-exp scores
45   block_mask = create_block_mask(
46     lambda b, h, q_idx, kv_idx: q_idx // chunk_size > kv_idx,
47     1, 1, q.shape[2], num_chunk
48   )
49   inter_out, inter_lse = flex_attention(
50     q, chunk_intra_k, chunk_intra_v,
51     scale=softmax_scale,
52     block_mask=block_mask,
53     return_lse=True
54   )
```

```

54
55     # Compute logits with
56     the current chunk's k, required separately due to causal masking
57     intra_lse
58     = einsum("batp, batp -> bat", q, intra_k) * softmax_scale
59
60     # Merge outputs
61     from previous chunks and current chunk (due to causal masking)
62     out =
63     merge_last_token_stable(inter_out, intra_v, inter_lse, intra_lse)
64     out = rearrange(out, "b a t p -> b t (a p)", a=num_head)
65     return z * out

```

Listing 1: Pseudo code for the training or prefilling modes of RAT. We use Pytorch's *flex attention* and *associative scan* for implementation.

```

1 def gen(z, g, q, k, v, chunk_start, num_head, cache):
2     """
3     Args:
4         z: (B, 1, D), output gate after sigmoid
5         g: (B, 1, D), forget gate after sigmoid
6         v: (B, 1, D), value vector
7         q, k: (B, 1, D), shared query and key vectors across heads
8         chunk_start: int, index of current chunk
9         cache: tuple of four tensors
10             lastkcache
11             : (B, 1, D), last token k in current chunk (for RNN-style update)
12             lastvcache
13             : (B, 1, D), last token v in current chunk (for RNN-style update)
14             kcache: (B, A, C, P) or
15                 (B, num_head, num_chunk, head_dim): cached k at each chunk's end
16             vcache: (B, A, C, P) or
17                 (B, num_head, num_chunk, head_dim): cached v at each chunk's end
18             # Note: KVCache is stored per chunk, not per token.
19     Returns:
20         out: (B, 1, D)
21     """
22     lastkcache, lastvcache, kcache, vcache = cache
23
24     # Intra-chunk RNN: Recurrent update within the current chunk
25     intra_k = g * lastkcache + (1.0 - g) * k
26     intra_v = g * lastvcache + (1.0 - g) * v
27     lastkcache.copy_(intra_k)
28     lastvcache.copy_(intra_v)
29
30     # Rearrange input for attention
31     intra_k = rearrange(intra_k, "b t (a p) -> b a t p", a=num_head)
32     intra_v = rearrange(intra_v, "b t (a p) -> b a t p", a=num_head)
33     q = rearrange(q, "b t (a p) -> b a t p", a=num_head)
34
35     # Apply RoPE
36     q, intra_k = apply_rope(q, intra_k)
37
38     # Update the current chunk's kvcache
39     kcache[:, :, chunk_start:chunk_start + 1] = intra_k
40     vcache[:, :, chunk_start:chunk_start + 1] = intra_v
41
42     # Inter-chunk
43     attention: standard attention over cached chunk representations
44     attn_out = scaled_dot_product_attention(
45         q, kcache[:, :, :chunk_start + 1], vcache[:, :, :chunk_start + 1], is_causal=False
46     )
47     out = rearrange(out, "b a t p -> b t (a p)", a=num_head)

```

```
return z * out
```

Listing 2: Pseudo code for the generation mode of RAT. We simply use the *flash attention* (Pytorch’s one). Note that KVCache of RAT is reduced from  $T$  to  $C$  compared to the attention module.

## A.2 Experiments

**Dataset** In our preliminary studies, we use the PG19 dataset [46], a long-form English book corpus with inherently long contexts. For the 1.3B model experiments, we adopt the FineWeb-Edu dataset [26], using its 100B-token randomly sampled version downloaded from the HuggingFace repository. To match the pretraining context length, we concatenate documents using a separator token. Note that web samples are usually very short, compared to the book dataset. For downstream evaluation, we consider a suite of classical commonsense reasoning benchmarks from the Eleuther AI evaluation harness [28], including PIQA [47], ARC-C [48], and HellaSwag [49]. In the LLaMA2 tokenizer, we observe that the inputs of these tasks typically contain fewer than 300 tokens. For the LongBench evaluation, in Table 7 we provide input length for each task, offering a rough indication of task difficulty with respect to input length. For SFT-based tasks, we have elaborated sequence lengths in the main text. As LongBench and SFT tasks often involve very long inputs, we apply truncation in the middle to preserve information at both the beginning and the end.

Table 7: We report the average input length and the 95th percentile input length of each task, measured in tokens using the LLaMA2 tokenizer. NQA (NarrativeQA), MQA (MultiFieldQA-en), HQA (HotpotQA), WQA (2Wiki-MultihopQA), MSQ (Musique), GR (GovReport), MN (MultiNews), TQA (TriviaQA), and RBP (RepoBench-P).

Task	Single-Document QA			Multi-Document QA			Summarization			Code Completion	
Name	NQA	Qasper	MQA	HQA	WQA	MSQ	GR	QMSum	MN	LCC	RBP
Avg.	36037	5780	8115	15329	8483	18555	12280	15980	3156	4307	14818
95th pctl.	77966	10164	14994	19755	16939	20066	25721	29069	7135	10401	31937

**200M model** We start with a 200M-parameter model in our preliminary study, with a model dimension of 1024, 12 transformer layers, and head dimension of 64. The rotary position embedding (RoPE) base is set to 10,000. We use the GPT2 tokenizer. Following Mohtashami and Jaggi [44], we repeat the PG19 training split five times to reach a total of 15B training tokens. The learning rate is scheduled using cosine annealing, starting at  $6.0 \times 10^{-4}$  and decaying to  $1.0 \times 10^{-6}$ , with a warm-up ratio of 10%. We use the AdamW optimizer with a weight decay of 0.1 and  $\beta = (0.9, 0.98)$ . Gradient clipping is applied with a threshold of 1.0, and the global batch size is set to 1M tokens. We explore training with three different context lengths: 8K, 16K, and 32K. Training these models on 4 H100 GPUs takes approximately 5 to 14 hours. In particular, the attention model requires up to 14 hours when the sequence length is  $T = 32768$ , whereas the RAT (L=16) model completes training in about 7 hours under the same setting.

**1.3B model** The 1.3B-parameter model uses a model dimension of 2048, 24 transformer layers, and a head dimension of 128, equipped with RMSNorm [50] and without bias. The RoPE base is also set to 10,000. The model parameters are initialized using a Gaussian distribution with a standard deviation of 0.02. We adopt the LLaMA2 tokenizer in the following studies. For pretraining, we use a cosine-annealed learning rate schedule starting at  $8.0 \times 10^{-4}$  and decaying to  $1.0 \times 10^{-6}$ , with 5% warmup. The global batch size is set to 2M tokens. We primarily train with a context window of 4K tokens and include additional experiments with a 16K context window, for which the RoPE base is increased to 500,000. Each model is trained on 16 H100 GPUs, requiring approximately 2 to 3 days to complete.

For LongBench evaluation, we follow the default prompts with greedy decoding for all tasks except summarization. For summarization, we apply a repetition penalty of 1.2 to address the common issue in pretrained-only models of generating repetitive outputs under instructional prompts. For SFT tasks, we train the models on the official training splits with an answer-only loss and evaluate them on the corresponding test sets. Although we explored different hyperparameters during the early experimentation, we observed that the relative trends remained largely stable. Thus, we fix the learning rate and batch size to  $(1.0 \times 10^{-5}, 128)$  for large datasets, and  $(1.0 \times 10^{-5}, 32)$  for the

smaller QMSum [30] task, following common practice for 1B-scale models. The weight decay is set as 0.01, and all other hyperparameters follow the pretraining setup. We sweep over the number of epochs and report the best result for each dataset and architecture. In practice, QA tasks typically converge in 1–2 epochs, while summarization benefits from slightly longer training.

## B Efficiency

### B.1 Latency

To supplement Fig. 2 in main text, we put the concrete latency number of a single layer in Table 8, Table 9, and Table 10.

Table 8: Single layer (including input and output projections) training time across different sequence lengths. The latency (ms) is tested on 200K tokens.

Model	4096	8192	16384	32768	65536	131072	262144
RNN	77.00	78.42	77.50	83.50	115.83	130.62	195.30
RAT(L=128)	150.19	150.76	156.65	154.52	159.94	165.07	206.46
RAT(L=64)	146.25	148.46	151.10	155.83	165.58	177.78	227.76
RAT(L=16)	150.08	153.63	158.98	173.89	202.00	249.79	378.11
Attention	122.06	176.44	277.61	474.90	877.14	1713.82	3417.48
Attention/RAT(L=16)	0.81×	1.15×	1.75×	2.73×	4.34×	6.86×	9.04×

Table 9: Single layer (including input and output projections) prefilling time across different sequences lengths. The latency (ms) is tested on 200K tokens.

Model	4096	8192	16384	32768	65536	131072	262144
RNN	24.93	24.75	25.32	27.09	30.54	39.40	56.16
RAT(L=128)	44.74	44.78	45.09	45.50	46.67	48.62	51.75
RAT(L=64)	43.46	44.27	44.27	44.83	47.08	50.83	57.38
RAT(L=16)	44.03	44.90	45.53	51.08	57.31	71.18	99.53
Attention	36.93	52.71	80.21	135.68	245.14	494.62	997.50
Attention/RAT(L=16)	0.84×	1.17×	1.76×	2.66×	4.28×	6.95×	10.02×

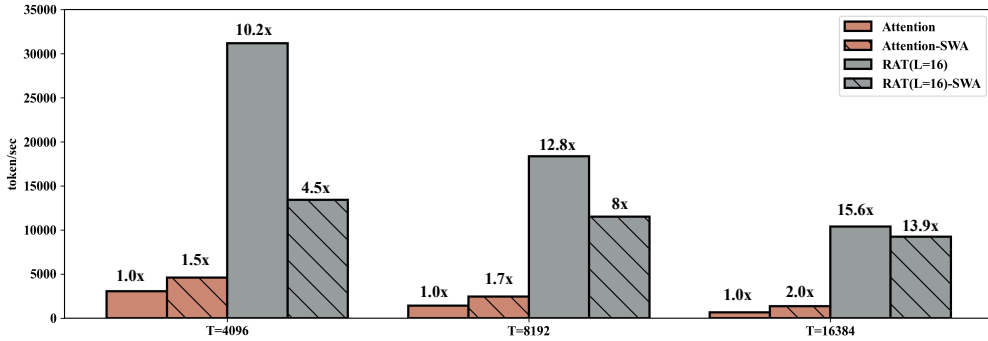


Figure 4: We measure the maximum throughput of the full 1.3B model for generating 1024 tokens under different prefilling lengths. For each total sequence length  $T$ , the prefilling length is set to  $T - 1024$ . For example,  $T = 4096$  corresponds to a prefilling of 3072 tokens, while  $T = 8192$  and  $T = 16384$  correspond to 7168 and 15360 tokens, respectively. When the sequence length increases, the maximum throughput ratio between RAT and attention rises from  $10.2\times$  to  $15.6\times$ , highlighting the strong efficiency advantage of RAT in long-context generation.

### B.2 Maximum throughput

As RAT also reduces cache memory usage, we report the maximum throughput of the full 1.3B model across different sequence lengths in Fig. 4. For example, RAT(L=16) achieves an approximately



Table 10: Single layer (including input and output projections) generation time at the specified position. The latency (ms) is tested on generating batches of tokens with  $B = 64$ ,  $B = 512$ , and  $B = 1024$ .

Model	4096	8192	16384	32768	65536	131072	262144
$B = 64$							
RNN	0.36	0.33	0.34	0.33	0.33	0.33	0.33
RAT (L=128)	0.62	0.60	0.61	0.63	0.66	0.66	0.68
RAT (L=64)	0.67	0.64	0.66	0.70	0.73	0.74	1.03
RAT (L=16)	0.62	0.65	0.64	0.68	1.04	1.82	3.42
Attention	1.15	1.73	3.33	6.66	12.94	26.8	OOM
$B = 512$							
RNN	0.35	0.34	0.33	0.33	0.34	0.34	0.33
RAT (L=128)	0.63	0.64	0.66	0.75	1.17	2.44	3.46
RAT (L=64)	0.70	0.68	0.74	1.16	2.41	3.44	6.69
RAT (L=16)	0.75	1.22	2.45	3.48	6.73	13.09	25.76
Attention	6.56	12.89	25.84	OOM	OOM	OOM	OOM
$B = 1024$							
RNN	0.36	0.36	0.35	0.35	0.35	0.36	0.35
RAT (L=128)	0.73	0.75	0.95	1.35	2.54	4.64	6.98
RAT (L=64)	0.74	0.94	1.35	2.48	4.67	7.02	13.45
RAT (L=16)	1.38	2.56	4.63	7.04	13.51	26.43	OOM
Attention	13.04	25.70	OOM	OOM	OOM	OOM	OOM

$10.2\times$  higher throughput than the baseline attention model at  $T = 4096$ , and improves further to  $15.6\times$  at  $T = 16384$ . Similarly, RAT (L=16) -SWA reaches  $4.5\times$ ,  $8.0\times$ , and  $13.9\times$  higher throughput over attention at  $T = 4096$ ,  $8192$ , and  $16384$ , respectively.

## C Accuracy

### C.1 Supplementary ablation study

All experiments here are conducted on the PG19 Book dataset with 200M-parameter models, and FLOPs are controlled for comparison.

**Reversed design of RAT** Instead of employing recurrence within each chunk, we also explored a reversed design that applies attention inside the chunk, followed by recurrence to capture long-range dependencies. For this reversed design, standard RoPE is sufficient. Regarding the parameter allocation, we found it crucial to retain the key vector in the attention module as a full tensor, as sharing it together with the query vector leads to a collapse into single-head attention. Thus, the final reversed design shares the query vector across attention heads, employs low-rank matrices for the projection used for output gate, and preserves full projections for both the forget gate and the key vector.

Results of the reversed design are put in Table 11. It can be observed that, under identical FLOP constraints, this design significantly underperforms RAT. We think this is because short-context dependencies are easier to capture and do not suffer from memory degradation, so using lightweight recurrence locally is more efficient. Long-context dependencies are harder and may require direct retrieval of distant information, where attention is more suitable. For example, to match the FLOPs budget of  $\mathcal{O}(T/64)$ , the reversed design requires chunk sizes of 128, 256, and 512 for sequence lengths of 8192, 16384, and 32768, respectively. With this small local window size, the long-range dependencies are attributed to the recurrence, thus leading to high perplexity. Only when we reduce the number of chunks to 16 does the perplexity drop below 14.00. Therefore, while the reversed design also allows for interpolation between attention and RNN (reducing to attention when  $L = T$ , and to RNN when  $L = 1$ ), we choose to focus on RAT due to its more efficient utilization of FLOPs.

**Comparison to FLASH [10]** As pointed out in Sec. 5, Hua et al. [10] also uses the concept of chunking; however, we adopt a fundamentally different framework, both in the components involved and in how the two outputs are combined. Specifically, Hua et al. [10] simply adds the outputs of inter-chunk and intra-chunk computations, whereas RAT organizes them hierarchically, applying recurrence over the key and value before inter-chunk attention. We argue that these differences lead to the weaker performance of Hua et al. [10], as shown in Table 13. First, as discussed above, RAT utilizes FLOPs more effectively than methods based on local attention, since its long-range dependencies must rely on memory-degrading components such as recurrence and linear attention. Second, we find that directly adding the outputs of softmax-based attention and linear attention introduces differences in output scale and potential representational conflicts, which may lower down the performance.

**Comparison to dilated attention** We discuss the difference between RAT and the design that interleaves recurrence and dilated attention [9] with the sliding pattern. First, from an efficiency perspective, RAT has advantages over dilated attention in both training and inference. During training, dilated attention reduces parallelism by the dilation rate, since tokens within the same dilation span attend to different KV vectors. In contrast, RAT allows tokens to share the same chunk-level representation, except within their own chunk. During inference, the sliding dilation pattern causes a memory issue, since the KV cache of all tokens must be stored, whereas RAT reduces the cache size proportionally to the chunk size. Second, in terms of accuracy, to match the FLOPs, we set the dilation rate to 64 for RNN-Dilated attention, since dilated attention occurs in only half of the layers. It can be seen from Table 14 that dilated attention performs poorly. We observed significantly slower convergence at the beginning of training, likely due to its lack of global perception.

Table 11: Perplexity results of the reversed design, where attention is applied within chunks and RNN is used across chunks. Experiments are conducted on the 200M model trained on the PG19 book dataset. Under the same FLOPs, it can be observed that RAT significantly outperforms its reversed counterpart.

Method	FLOPs	T=8192	T=16384	T=32768
RAT (L=128)	$\mathcal{O}(T/128)$	13.57	13.44	13.66
RAT (L=64)	$\mathcal{O}(T/64)$	13.42	13.34	13.39
RAT-Reversed (C=128)	$\mathcal{O}(T/128)$	14.53	14.35	14.37
RAT-Reversed (C=64)	$\mathcal{O}(T/64)$	14.21	14.06	14.02
RAT-Reversed (C=16)	$\mathcal{O}(T/16)$	13.69	13.48	13.50
Attention	$\mathcal{O}(T)$	13.26	13.10	13.19

Table 12: Pretraining and downstream evaluation results of 1.3B models using either RoPE or NoPE positional encodings. RoPE is used in the main text, while NoPE is trained for investigating length extrapolation. Notably, NoPE achieves reasonable performance even at the 1B model scale with only 100B training tokens.

Method	PE	Pretrain PPL	HellaSwag acc_norm	LAMBADA acc	PIQA acc_norm
Attention-SWA	RoPE	7.61	57.1	48.0	72.7
RAT (L=16) -SWA	RoPE	7.57	57.9	49.3	73.9
Attention-SWA	NoPE	7.69	56.4	47.3	72.7
RAT (L=16) -SWA	NoPE	7.63	56.8	47.8	73.7

Table 13: Performance of different chunk-based designs with  $T = 16384$  and FLOPs  $\mathcal{O}(T/64)$ .

Method	Intra-chunk	Inter-chunk	Organization	PPL
RAT (L=64)	Recurrence	Attention	Hierarchically	<b>13.34</b>
RAT-Reversed (C=64)	Attention	Recurrence	Hierarchically	14.06
FLASH (C=128)	Attention	Linear attention	Add together	14.4

Table 14: Performance compared to dilated attention with sliding patterns under the same FLOPs.

Method	PPL
RNN-Dilated attention	15.22
RAT (L=128)	13.44

## C.2 Length generalization

Because of the use of softmax-based attention and RoPE at the inter-chunk level, it is reasonable to expect that RAT may also face challenges in length generalization, where the model is trained on short sequences but evaluated on much longer ones. To study this, we consider SWA variants using either RoPE or NoPE for attention and RAT, following recent practices that interleave attention with local attention modules and apply positional encodings only in the local attention. This design has been adopted in practice and has shown promising results [22].

As shown in Fig. 5, the RNN performs very steadily as the test sequence length increases. However, within the training context, it has the highest loss among all models. With RoPE, both Attention-SWA and RAT (L=16) -SWA experience a sharp increase in loss when the sequence length goes beyond 6000. The increase is more severe in the attention model than in the RAT variant. This is likely because RAT reduces the effective attention span by attending only to inter-chunk positions, which may offer better robustness to extrapolation.

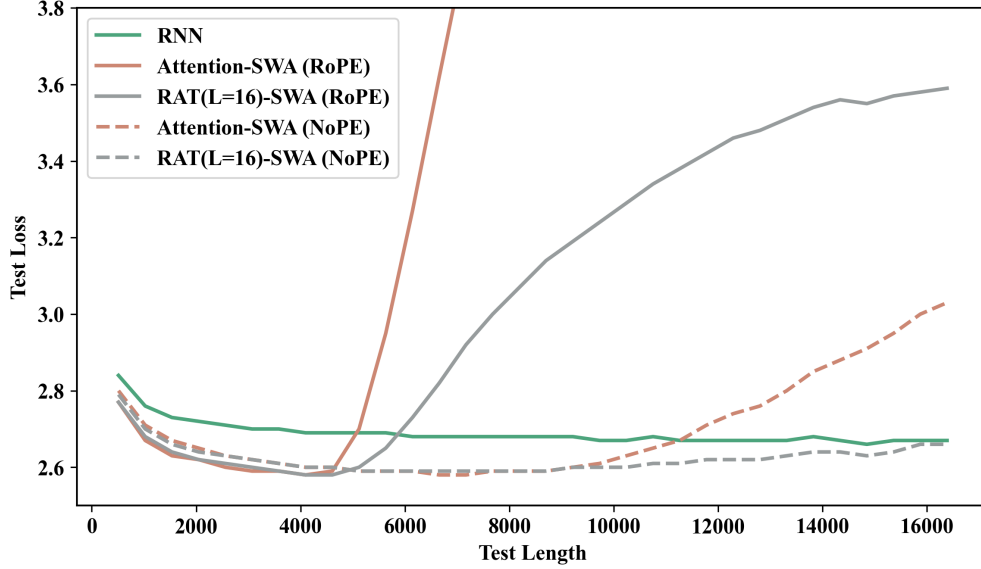


Figure 5: Evaluation at different test lengths for pretrained models trained with a 4K context window. RAT(L=16)-SWA with NoPE achieves the best overall performance, exhibiting strong generalization up to  $T=16384$  while maintaining low loss within the training context.

We also pretrain NoPE versions, where no positional encodings are used in attention or RAT layers. Interestingly, these NoPE models show reasonable performance, as reported in Table 12. While their pretraining perplexities are higher than those of the RoPE variants, the gap remains small, especially considering the 1.3B model size and 100B-token training budget. To further verify this, we evaluate the models on several commonsense reasoning tasks and obtain promising results. We expect that NoPE will perform even better with larger models and longer training. In terms of length extrapolation, using NoPE significantly improves the robustness for both Attention-SWA and RAT(L=16)-SWA. Among them, RAT(L=16)-SWA with NoPE shows the most stable performance, maintaining low loss even at a sequence length of 16,384.

In conclusion, we find that RAT can outperform the attention module in length generalization, both with RoPE and with NoPE. Still, the problem is not fully solved, as none of the models reach the stability level of the simple RNN. While many techniques have been proposed to improve length extrapolation in attention models, they should also be considered for RAT, as RAT essentially redirects attention from every position to inter-chunk locations. For example, RoPE extrapolation in the attention module can be improved using methods from Peng et al. [51], bloc97 [52], and NoPE extrapolation has been studied in Wang et al. [53], which points out that NoPE still has a context length limit, though it performs better than RoPE. Their work links the failure to shifts in attention distributions and proposes tuning the temperature of attention heads to improve extrapolation. We believe such methods could also be applied to RAT, and leave further exploration of these techniques to future work.

### C.3 Needle-in-Haystack (retrieval ability)

To evaluate retrieval capabilities—an area where attention-based architectures are known to excel, and where RNNs typically fall short—we conduct experiments on the Needle-in-Haystack tasks. In these tasks, a "needle" (e.g., a magic number or UUID) is embedded within irrelevant passages, noisy text, or mixed with multiple key-value pairs. Each key-value pair is presented as a short identifier (the key) followed by its associated value, and the model is prompted to retrieve the correct value given a specific key.

We adopt the RULER benchmark [32] and evaluate a range of Needle-in-Haystack task configurations. Specifically, task `single_1` involves retrieving a specific number from a background filled with repeated noise. In `single_2`, the background is replaced with natural stories. `single_3` increases the difficulty by requiring retrieval of a long and complex UUID. The `multikey` tasks are more

challenging than the single-key ones, as they introduce multiple such key-value pairs into the context. In particular, `multikey_2` and `multikey_3` consist almost entirely of densely packed key-value pairs, among which only a single key is queried at the end. This makes the task especially challenging, as the model must retrieve the correct item from a highly cluttered input full of distractors. And `multikey_3` further incorporates the complex UUID format. In the `multiquery` and `multivalue` settings, the model is required to resolve multiple retrieval targets, either by answering several distinct queries or by retrieving all values associated with a single key. For detailed definitions of each task, we refer the reader to the benchmark documentation.

During evaluation, we observed that models may fail to interpret certain prompts correctly. For instance, prompts like *"A special magic number is hidden within the following text. Make sure to memorize it. I will quiz you about the number afterwards."* can cause failures even in attention-based models, especially on the harder `multikey` tasks. To mitigate this, we apply a light, one-round supervised fine-tuning stage before evaluation to adapt the models to the instruction patterns. We generate 1000 synthetic training samples for each of the 8 tasks, resulting in a total of 8000 examples disjoint from the validation sets. The models are trained on this dataset for one round and then are evaluated directly on all 8 tasks. This procedure yields a fairer and more stable comparison. As shown in Table 6, RNNs perform reasonably well on the simpler tasks (`single_1`, `single_2`), but their performance drops to near zero on the harder ones. Attention-based models perform consistently well, benefiting from their ability to access all previous tokens directly. RAT(L=16) achieves results close to full attention, especially in numeric tasks. However, it struggles on UUID tasks due to their complexity and the use of exact match scoring (`single_3`, `multikey_3`). Meanwhile, RAT(L=64) falls between RNNs and RAT(L=16), as expected given its partial access to long-range context.

These results are consistent with the underlying architecture designs: attention provides full direct access to all past tokens, RNNs compress all past information into a hidden state, while RAT compresses part of the history but also retains direct access at the chunk level. As a result, RAT naturally exhibits retrieval capabilities that lie between those of attention and RNNs.

## D Broader Impacts

Enhancing the efficiency of Large Language Models (LLMs) can significantly reduce computational resources and energy consumption, benefiting the environment and democratizing access to advanced AI technologies. However, increased efficiency could also lead to greater dissemination of disinformation and the creation of deepfakes, posing risks to public trust and security and potentially reinforcing existing biases that impact specific groups unfairly. This research aims to promote the responsible development and deployment of LLMs, maximizing societal benefits while acknowledging potential harms.

## E License information

- FineWeb-Edu (dataset): Open Data Commons License Attribution family.  
Link: <https://huggingface.co/datasets/HuggingFaceFW/fineweb-edu>
- LongBench (dataset and code): MIT License.  
Link: <https://github.com/THUDM/LongBench>
- NarrativeQA (dataset): Apache License 2.0.  
Link: <https://github.com/deepmind/narrativeqa>
- QMSum (dataset): MIT License.  
Link: <https://github.com/Yale-LILY/QMSum>
- WikiSum (dataset): Custom license (unspecified).  
Link: <https://huggingface.co/datasets/d0rj/wikisum>
- lm-evaluation-harness (code): MIT License.  
Link: <https://github.com/EleutherAI/lm-evaluation-harness>
- RULER benchmark (code): Apache 2.0 License.  
Link: <https://github.com/NVIDIA/RULER>